ELSEVIER

Polymer 42 (2001) 2585–2595

polymer

www.elsevier.nl/locate/polymer

Mechanical properties and interrelationships of poly(methyl methacrylate) following hydration over saturated salts

R.P. Kusy[a,b,c,d,*], J.Q. Whitley[d], S. Kalachandra[d,e]

[a]*Department of Orthodontics, University of North Carolina, Chapel Hill, NC 27599, USA*
[b]*Department of Biomedical Engineering, University of North Carolina, Chapel Hill, NC 27599, USA*
[c]*Curriculum in Applied and Material Sciences, University of North Carolina, Chapel Hill, NC 27599, USA*
[d]*Dental Research Center at University of North Carolina, Chapel Hill, NC 27599, USA*
[e]*Department of Chemistry at Virginia Polytechnic Institute, Blacksburg, VA 24061-0344, USA*

Received 21 April 2000; received in revised form 3 August 2000; accepted 4 August 2000

Abstract

Three types of specimens were machined from a model unfilled linear poly(methyl methacrylate) (PMMA), which was nominally 1.5 mm thick. After pre-condition annealing and pre-drying, the specimens were equilibrated at one of eight relative humidities (RH) at 22 or 37°C. Thereafter, the parallelepipeds were deflected in 3-point bending, the dumbbells were pulled in tension or deformed using a Knoop (HK) microhardness indenter, and the disks were deformed using a Vickers (HV) microhardness indenter. As the RH increased from 0 to 100%, the samples exponentially sorbed 2% w/w of water. Elastic moduli in bending and tension (E_B and E_T), ultimate tensile strength (UTS), and hardnesses (HV and HK) were inversely and linearly dependent on water uptake ($p < 0.001$). Strain at UTS (ε_{UTS}) was independent of weight change; whereas, strain at fracture (ε_F) was directly and linearly dependent on water uptake ($p < 0.02$). Under these equilibrium conditions of sorption, no evidence was found that sustained the concept that a break in mechanical properties occurred at about 1% sorption as a result of plasticization leading to clustering. After logarithmic transformations of selected mechanical properties, linear correlations were found between HV versus E_B ($p < 0.02$) and strength (UTS or YS) versus HV ($p < 0.001$). The results paralleled the relationship found for pure face-centered-cubic (FCC) metals in the former case and was coincident with the relationship for FCC metals in the latter. These interrelationships suggest that the effects of plastic anisotropy are absent in hydrated PMMA and that water continues to facilitate long-range elastic interactions.

Keywords: Interrelationships; Plasticization; Poly(methyl methacrylate)

1. Introduction

For fifty years acrylics have been a mainstay of dentistry — first as a replacement for vulcanite in dentures [1–4], then as denture repair and reliner materials [5–7], and most recently as the basis for composite restorations [8–12]. Not long after acrylics were introduced, problems were noted that were associated with absorbed water [13–18], residual monomer [19], and the general leaching of unreacted ingredients [5,11,18]. These chemical changes were accompanied by decreases in rigidity [20,21], strength [20–26], and hardness [9,24,27,28] that ultimately could affect fatigue strengths [29] via midline fractures of dentures [30], change in the compliance of denture reliners [5], wear of occlusal surfaces of composites [11,12], and even degradation of relatively unstressed class V restorations [31]. Indeed, many of the shortcomings of appliances (albeit to a lesser degree in the crosslinked acrylics [32]) could be attributed to the polar nature of its homologues and so its hydrophilicity.

Literally hundreds of papers have been written concerning the water sorption of acrylics and include studies of chemical composition [4,25,33–35], molecular weight [18], plasticizers [6,36,37], reinforcement fillers [4,7,38,39], crosslinking agents [7,32], and barrier coatings [40]. The consensus of these investigations may be generalized as follows: (1) glassy acrylics such as poly(methyl methacrylate) (PMMA) typically sorb ca 2% w/w water [22,41]; (2) the process is diffusion controlled in which the constant for desorption is greater than that for absorption [42,43]; (3) within the physiologic region of interest water sorption is not strongly temperature dependent [13]; (4) mechanical properties (e.g. transverse rupture strength, ultimate tensile strength, and microhardness) decrease with water uptake [18,22]; and (5) a break appears in mechanical

* Corresponding author. Tel.: +1-919-966-4598; fax: +1-919-843-8864.
E-mail address: rkusy@bme.unc.edu (R.P. Kusy).

0032-3861/01/$ - see front matter
PII: S0032-3861(00)00613-3

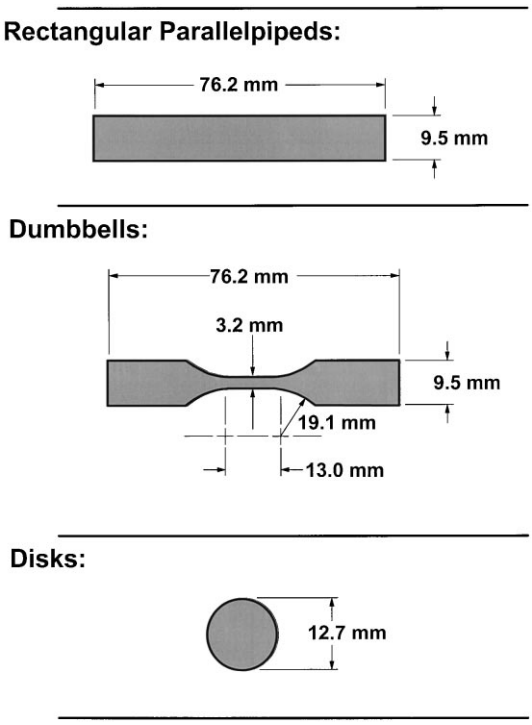

Fig. 1. Schematic drawings showing the nominal specimen geometries of 1.5 mm thick poly(methyl methacrylate) (PMMA) specimens of Plexiglas G™ that were used in these hydration experiments.

characteristics at ca 1% w/w water uptake that corresponds to clustering versus plasticization [18]. In the most comprehensive studies, the previous literature deduced these facts from equilibrated dry and fully hydrated states but non-equilibrated intermediate sorption states. Thus, when the test samples were unconstrained, the dry and hydrated states had uniform strain states from swelling. However, for those samples that were in water for a time less than that required for equilibrium to be established, the sorption profile at different points from the surface to the center varied greatly. Indeed, such samples that had been preconditioned in the dry state and then immersed in water would develop a variable sorption profile and likely different diffusion constants. As a consequence, a strain gradient would result that could affect the outcomes of mechanical tests.

The present work seeks to eliminate such residual stresses by equilibrating samples in either a uniformly preconditioned or an as-received state at either room or oral cavity temperature using saturated salt solutions. Having established a uniform profile of water concentration, the strain states associated with flexural, tensile, and hardness tests are imposed on the appropriate specimen geometries. Two hypotheses will be tested: (1) that up to about 50% sorption, water acts predominantly as a plasticizer; and (2) that larger amounts of water additionally result in the formation of molecular clusters. The first will be tested by checking whether specific mechanical properties continuously decrease to about 50% saturation (i.e. ca 1% w/w water uptake). The second will be tested by checking whether a

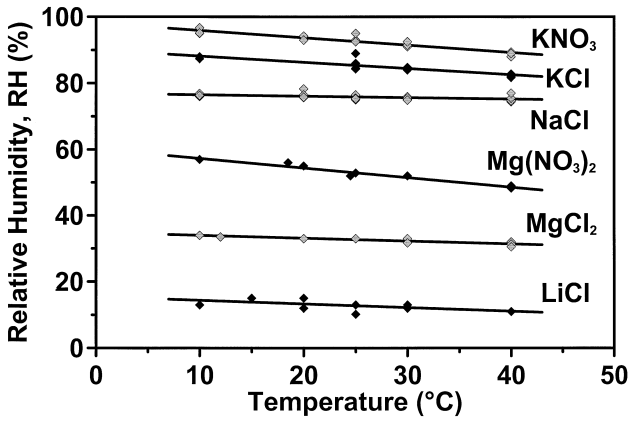

Fig. 2. Influence of temperature on the relative humidity (RH) for six supersaturated salt solutions [46,47]. Note that RH is independent of temperature between 10 and 40°C.

discontinuity and/or a change occurs in specific mechanical properties above 1% w/w as the plasticizing action of water gives way to the formation of clusters.

2. Material and methods

A commercially available, linear, and unfilled poly(methyl methacrylate) (PMMA), Plexiglas G™ (Rohm and Hass Co., Philadelphia, PA), was selected as a model material having a viscosity average molecular weight (M_V) equal to 1.2×10^6 [44]. The nominally 1.5 mm thick sheet stock was machined into three types of samples (Fig. 1).

Samples were primarily pre-conditioned by annealing in vacuum at 70°C for 24 h [45], although some specimens were conditioned from the as-received state without preconditioning. Such an annealing schedule satisfies Smith's observation that, provided cure times are more than 8 h at 70°C, the residual monomer is maintained below critical levels (3% w/w) [19]. Typically, residual monomer is $<$0.2% w/w. After the samples were pre-dried at 22°C in vacuum (ca 10^{-3} Torr) to 0% RH, they were then equilibrated at one of two temperatures (22°C [▲ and ●] or 37°C [▽, ○, and ◇]) and at one of eight relative humidities (RH): 0 (in vacuum), 100 (in distilled water), and nominally 13, 33, 52, 76, 85, and 92% RH over various inorganic salts (Table 1). The actual RHs for these two temperatures (Table 1) were determined by extrapolating data in the literature for temperatures that bracketed 22 and 37°C (Fig. 2) [46,47]. For each saturated salt solution, the RH was largely independent of temperature within this range. For the three test geometries, six specimens at each conditioning temperature and RH were monitored during equilibration to determine when constant weight had been obtained (Fig. 3). After equilibration, the rectangular parallelepipeds and dumbbells were measured ($\pm$0.001 mm) three times per dimension using a Sony μ-Mate digital caliper (Sony Magnescale America, Inc., Orange, CA). Three testing methods were

Table 1
Actual relative humidity (%) tested

Saturated salt solutions	Conditioning temperature (°C)	
	22	37
LiCl	13	12
$MgCl_2$	33	32
$Mg(NO_3)_2$	54	49
NaCl	76	75
KCl	86	83
KNO_3	93	90

used to evaluate the mechanical properties of these samples: bending, tensile, and hardness.

The bending modulus (E_B) of each parallelepiped was determined using a three-point bending apparatus (outer span of 50.8 mm) that was attached to an Instron universal testing machine (Instron Corp., Canton, MA). A crosshead speed of 0.1 cm/min was used to test six samples at each RH of the annealed specimens (Table 2). A second bending test method ("piston-on-ball") [48–50] was attempted but found unsuitable for these plastic samples.

Using an Instron universal testing machine, dumbbell samples were mounted with a nip-to-nip distance of 35 mm and tested in tension at a crosshead extension speed of 0.1 cm/min. To measure strain, one of two extensometers (10% [● and ○] or 50% [▲ and ▽]) with a 12.7 mm gage length was attached within the necked region of each sample. For each RH, six samples were tested for each as-received or annealed pre-conditioning treatment (Table 2). Because the 10% extensometer was five times more sensitive, both extensometers were calibrated using its calibration constant. Using that scalar, each tensile modulus (E_T), ultimate tensile strength (UTS), strain at UTS (ε_{UTS}), and strain at break (ε_F) was calculated.

Prior to tensile testing, the Knoop hardness (HK) was determined in the gripping region of each dumbbell sample using a Kentron microhardness tester (Kent Cliff Labs, Peekskill, NY). An indenter load of 75 g was used with each dumbbell sample (Table 2). For each RH of the annealed disks (Table 2), the Vickers hardness number (VH) was calculated at five locations on six samples using the same microhardness instrument but with a heavier indenter load of 200 g.

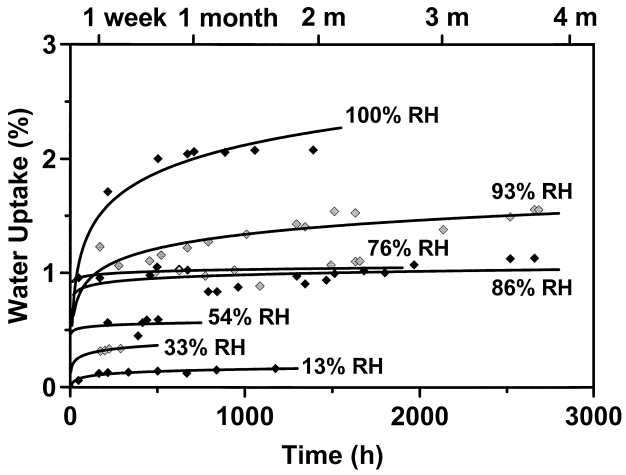

Fig. 3. Typical absorption curves of one annealed parallelepiped at 22°C for 13, 33, 54, 76, 86, 93, and 100% RH. For this sheet thickness (1.5 mm), equilibration always occurred in about two months.

Means and standard deviations were calculated for the water uptake, E_B, E_T, UTS, ε_{UTS}, ε_F, HK, and HV. Exponential regressions were determined for water uptake against RH, and linear regressions were determined for E_B, E_T, UTS, ε_{UTS}, ε_F, HK, and HV against both RH and water uptake. For each of these regressions the statistical significance (p) was deduced from the correlation coefficient (r) and the number of data points (n). Scatter diagrams (◇ and ○) were determined for the as-received minus the annealed pretreatments for E_T, UTS, ε_{UTS}, and HK against RH at 37°C. After the X- and Y-axes were logarithmically transformed, the interrelationships of hardness (HV or HK) versus modulus (E_B, E_T, or E_K) and strength (UTS or YS) versus hardness (HV or HK) were determined for PMMA, ductile metals, and covalent or ionic crystals.

Table 2
Tests performed (+) after a pre-conditioning treatment at a specific conditioning temperature (cf. Table 1)

Tests (measurements)	Pre-conditioning treatment	Conditioning temperature (°C)	
		22	37
3-pt Bending (E_B)	As-received[a]	–[b]	–
	Annealed[c]	+	+
Tensile testing (E_T,	As-received	+	+
UTS, ε_{UTS}, ε_F)	Annealed	–	+
Knoop Hardness (HK)	As-received	+	+
	Annealed	–	+
Vickers Hardness (HV)	As-received	–	–
	Annealed	+	+

[a] Not heat treated.
[b] No tests were performed.
[c] Heat treated in vacuum at 70°C for 24 h [45].

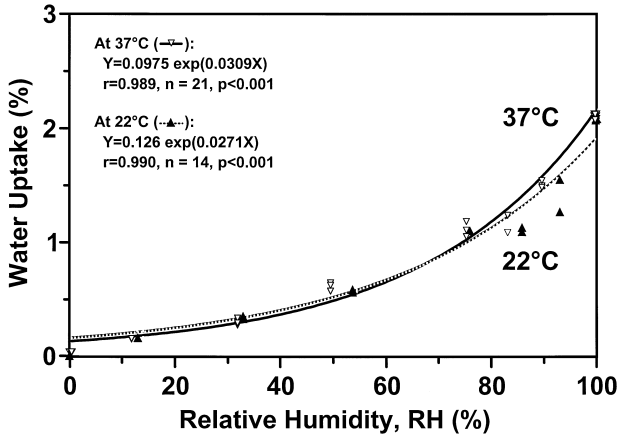

Fig. 4. Relationship of equilibrium water uptake as a function of RH for annealed PMMA. Note the temperature independence for sorption at 22°C (▲) and 37°C (▽), since the unhydrated glass transition temperature (105°C) [51] is substantially higher than either conditioning temperature.

3. Results

3.1. Water sorption

Equilibrium water uptake increased exponentially with RH to a maximum of about 2.1% w/w at 100% RH ($p < 0.001$; Fig. 4). At the equilibrated condition, the water uptake appeared independent of conditioning temperature for parallelepiped- and disk-shaped specimens (Table 3).

3.2. Annealed samples

The results at 22°C (▲) were generally higher than the results at 37°C (▽ and ○). The bending modulus (E_B) was inversely and linearly related to RH ($p < 0.001$; Fig. 5). The values of E_B ranged from 3.4 ± 0.1 to 2.7 ± 0.0 GPa for samples conditioned at 22 and 37°C, respectively ($p < 0.001$; Table 4). Each tensile modulus (E_T) decreased as RH increased (Fig. 5). The E_T for annealed samples decreased from 3.2 ± 0.5 to 2.1 ± 0.0 GPa (Table 4). As RH increased, the UTS decreased from 76 ± 1 to 61 ± 1 MPa ($p < 0.001$; Table 4). Strain at UTS (ε_{UTS}) was independent of RH, the overall values averaging 0.070; strain at break (ε_F) scattered widely from 0.06 at 0% RH to 0.56 at 100% RH (Fig. 5). For samples that were conditioned at 37°C, HK decreased from 21 ± 1 kg/mm^2 at 0% RH to 18 ± 1 kg/mm^2 at 100% RH; whereas, HV decreased from 25 ± 0 to 19 ± 0 kg/mm^2 (Table 4). Trends were similar when the same measurements were plotted against water uptake (Fig. 6), wherein each dotted line represents the solubility limit of water in PMMA.

3.3. As-received samples

When dumbbell specimens were conditioned without a stress-relieving heat treatment, the E_T, UTS, ε_{UTS}, and HK followed the same trends as the annealed data (cf. Fig. 5). Fig. 7 summarizes the outcomes at two temperatures in which the data at 22°C (●) is once again slightly but not significantly greater in magnitude than the data at 37°C (○). In the case of E_T at 0 and 100% RH, for example, the values decreased from 2.9 ± 0.3 to 2.4 ± 0.1 GPa at 22°C and from 2.8 ± 0.1 to 2.4 ± 0.1 GPa at 37°C (Table 5). The ε_{UTS} was the only property that was independent of RH, for which the values equaled 0.07 ± 0.00 at both 22 and 37°C (Table 5).

Table 3
Summary of the water uptake (%) for various geometries of annealed samples

Conditioning temperature (°C)	Actual relative humidity (%)	Water uptake (%)		
		For the parallelepiped specimens (E_B tests)	For the dumbbell specimens (E_T, UTS, ε_{UTS}, ε_F, and HK tests)	For the disk-shaped specimens (HV tests)
22	0	0.00 ± 0.00[a]		0.00 ± 0.00
	13	0.16 ± 0.01		0.16 ± 0.01
	33	0.33 ± 0.01		0.35 ± 0.01
	54	0.58 ± 0.01		0.56 ± 0.01
	76	1.10 ± 0.01		1.10 ± 0.02
	86	1.13 ± 0.01		1.09 ± 0.02
	93	1.55 ± 0.01		1.27 ± 0.02
	100	2.08 ± 0.01		2.13 ± 0.04
37	0	0.00 ± 0.00	0.00 ± 0.00	0.00 ± 0.00
	12	0.12 ± 0.00	0.12 ± 0.01	0.12 ± 0.01
	32	0.30 ± 0.01	0.23 ± 0.01	0.24 ± 0.03
	49	0.59 ± 0.00	0.54 ± 0.00	0.61 ± 0.01
	75	1.16 ± 0.01	1.08 ± 0.02	1.02 ± 0.02
	83	1.06 ± 0.01	1.06 ± 0.01	1.21 ± 0.02
	90	1.48 ± 0.01	1.46 ± 0.02	1.52 ± 0.02
	100	2.06 ± 0.01	2.06 ± 0.01	2.11 ± 0.04

[a] Means ± standard deviation are reported for six data points.

Table 4
Summary of the mechanical properties of annealed samples

Conditioning temperature (°C)	Actual relative humidity (%)	For the parallelepiped specimens	For the dumbbell specimens					For the disk-shaped specimens
		Modulus, E_B (GPa)	Modulus, E_T (GPa)	Ultimate tensile strength, UTS (MPa)	Strain at UTS, ε_{UTS} (mm/mm × 100)	Strain at break, ε_F (mm/mm × 100)	Knoop Hardness, HK (kg/mm^2)	Vickers Hardness, HV (kg/mm^2)
22	0	3.27 ± 0.11[a]						25.1 ± 0.5
	13	3.35 ± 0.08						24.0 ± 0.4
	33	3.26 ± 0.03						24.0 ± 0.7
	54	3.18 ± 0.07						23.7 ± 0.5
	76	3.20 ± 0.02						22.0 ± 0.2
	86	3.20 ± 0.02						21.7 ± 0.2
	93	3.09 ± 0.05						21.8 ± 0.6
	100	2.85 ± 0.04						19.4 ± 0.2
37	0	3.30 ± 0.02	2.94 ± 0.50(5)	75.7 ± 0.7	7.1 ± 0.4	13.1 ± 4.3	20.9 ± 0.5	24.6 ± 0.3
	12	3.29 ± 0.05	3.23 ± 0.49(3)	74.8 ± 0.8	7.0 ± 0.5	10.7 ± 3.0	21.2 ± 0.3	23.7 ± 0.4
	32	2.96 ± 0.09	3.02 ± 0.33(4)	73.2 ± 1.0	6.7 ± 0.6	15.6 ± 12.1	21.0 ± 0.4	23.7 ± 0.3
	49	3.13 ± 0.04	2.60 ± 0.13	70.6 ± 0.6	7.3 ± 0.2	13.9 ± 7.5	20.3 ± 0.9	22.0 ± 0.4
	75	3.05 ± 0.03	2.28 ± 0.15	67.8 ± 0.6	7.3 ± 0.4	12.7 ± 5.9	19.8 ± 0.4	21.3 ± 0.5
	83	3.05 ± 0.02	2.22 ± 0.19(4)	69.6 ± 0.9	7.3 ± 0.2	11.8 ± 2.9	18.9 ± 0.3	21.3 ± 0.5
	90	2.73 ± 0.06	2.13 ± 0.04(3)	64.9 ± 0.8	6.9 ± 0.6	16.9 ± 10.9	17.9 ± 0.3	21.1 ± 0.6
	100	2.69 ± 0.03	2.31 ± 0.29(3)	60.7 ± 0.5	6.4 ± 0.5	31.1 ± 14.7	17.5 ± 0.5	19.4 ± 0.4
37[b]	0		2.88 ± 0.06	76.0 ± 0.7	6.8 ± 0.3			
	100		2.46 ± 0.07	58.6 ± 2.5	5.6 ± 1.6			

[a] Means ± standard deviation are reported for six data points, except for those indicated in parentheses.
[b] Retested using a 10% extensometer instead of a 50% extensometer.

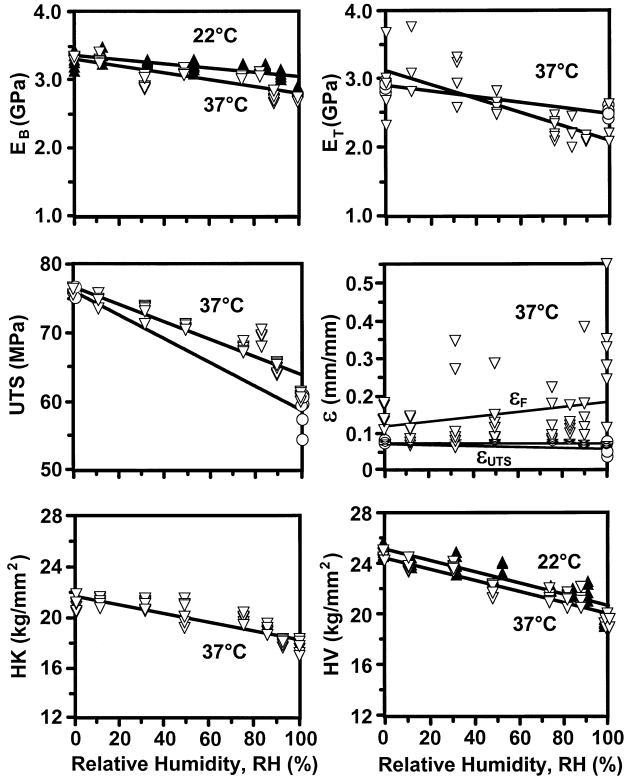

Fig. 5. Plots of bending and tensile moduli (E_B and E_T), ultimate tensile strength (UTS), strains at UTS and break (ε_{UTS} and ε_F), and Knoop and Vickers hardnesses (HK and HV) as a function of RH and conditioning temperatures (22°C [▲] and 37°C [▽ and ○]) for annealed PMMA parallelepipeds, dumbbells, and disks (cf. Tables 2 and 4). For the tensile tests, these same circular and triangular symbols also differentiate the data obtained using a 10 and 50% extensometer, respectively. All regressions were highly statistically significant ($p < 0.001$), except for ε_F and ε_{UTS} against %RH ($p =$ NS).

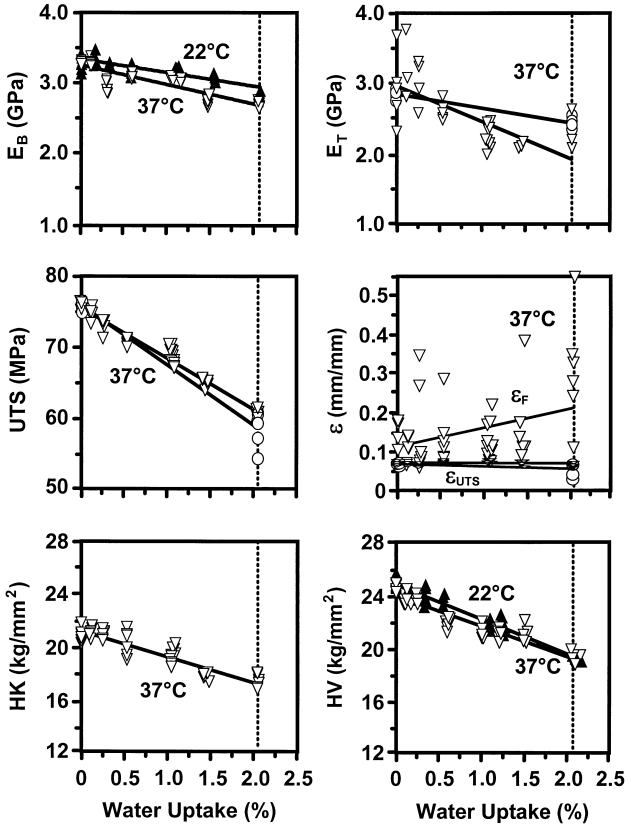

Fig. 6. Plots of mechanical properties as a function of water uptake and conditioning temperatures (cf. symbols of Fig. 5) for annealed PMMA parallelepipeds, dumbbells, and disks (cf. Tables 2 and 4). Here each dotted line represents the solubility limit of water in PMMA (cf. Table 3). All regressions were highly statistically significant ($p < 0.001$), except for ε_F against water uptake ($p < 0.02$) and ε_{UTS} against water uptake ($p =$ NS).

4. Discussion

4.1. Scatter diagrams of properties following preconditioning treatments

Based upon the results of the common properties (cf. Figs. 5 and 7), the differences between four properties (ΔE_T, ΔUTS, $\Delta\varepsilon_{UTS}$, ΔHK) were determined in the annealed versus the as-received precondition (cf. dumbbell specimens at 37°C, Tables 4 and 5). Based on these scatter diagrams (Fig. 8), no statistically significant differences were seen among these four properties ($p =$ NS), except when the ΔE_T against %RH data were compared at 37°C (◇) for the two extensometers. The similarity between annealed and as-received data was quite unexpected because the presence of residual stresses in the as-received material presumably should have had a negative influence on the properties — and particularly on ε_F [52]. Perhaps under these equilibrium conditions of hydration these as-received specimens were sufficiently plasticized to relax, thereby dissipating any pre-existing residual stresses [53]. Moreover, since equilibrium conditions were imposed, no water-induced strain gradients were present either. Thus, the as-received and annealed data could have been grouped, although they remain ungrouped in the discussion that follows.

4.2. Comparisons with the literature

In conventional terms, PMMA is a glassy polymer that, when starting from the dry state, absorbs about 2.1% w/w water at equilibrium [5,18,22,36,41,42,54]. Unlike the hydration conditions between 0 and 100% RH, the equilibrium conditions at 0 and 100% RH have been easy for many researchers to establish and replicate. Assuming a planar slab model, only the thickness has influenced the time required to establish the selected equilibrium concentration [55]. Braden described the kinetics that govern such water sorption (including the diffusion constants) and published a chart that conveniently permits one to calculate the time required to attain 99% saturation as a function of thickness [42]. In the present case, about 500 h and certainly no more than a month is required to attain equilibrium at 22°C and 100% RH. For a 1.5 mm thick slab, Braden predicted 250 h, which agree within a factor of two. Braden

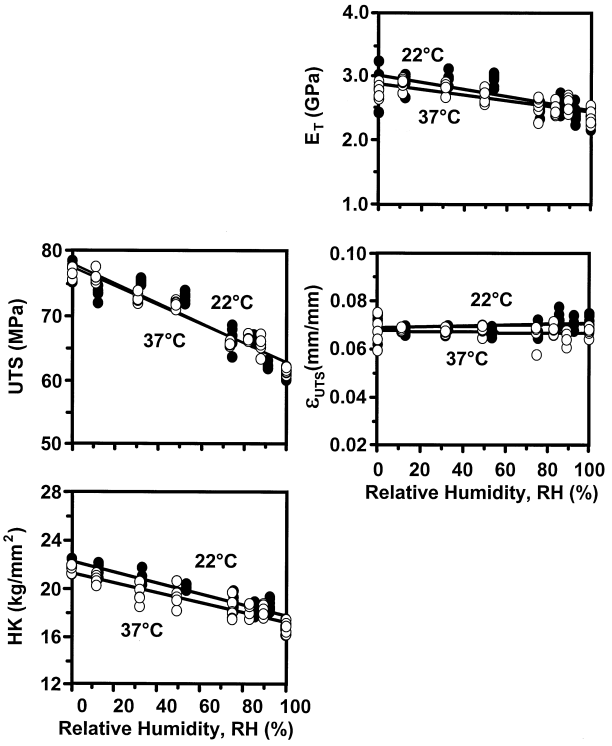

Fig. 7. Plots of selected mechanical properties as a function of RH and conditioning temperatures (22°C [●] and 37°C [○]) for as-received PMMA dumbbells (cf. Tables 2 and 5). For the tensile tests, these symbols also represent data obtained by using a 10% extensometer. All regressions were highly statistically significant, except for ε_{UTS} against %RH (p = NS). To differentiate these two conditioning temperatures, the scale of ε_{UTS} has been enlarged fivefold over that of Figs. 5 and 6.

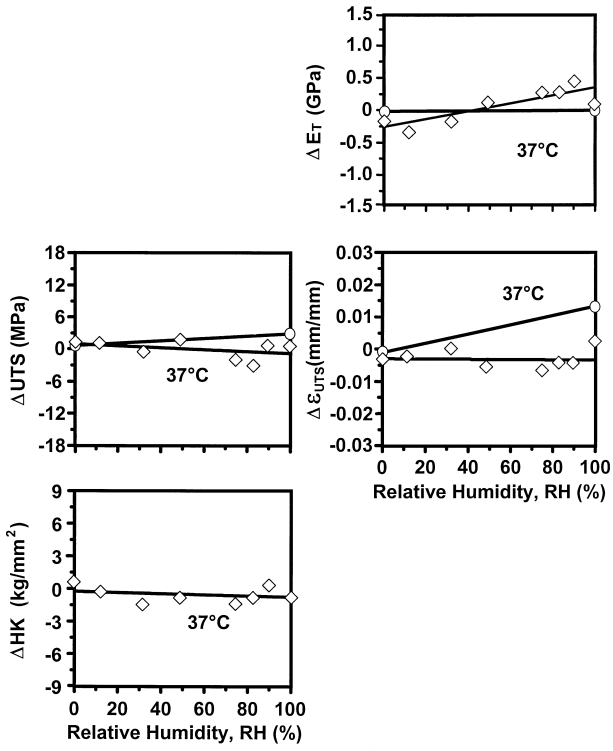

Fig. 8. Scatter diagrams of tensile and HK tests (i.e. ΔE_T, ΔUTS, $\Delta\varepsilon_{UTS}$, and ΔHK) as a function of RH for the as-received minus the annealed preconditioning treatments. All regressions were not significant (◇ and ○; p = NS), except in one series of E_T tests (◇; $p < 0.01$). Because the differences between treatments were small, the data could have been grouped.

et al. [43] also illustrated that sorption was a slower process than desorption and provided details of the mechanism. Finally, just as Brauer and Sweeney's earlier work had shown over a broader range of temperature (4–60°C) [13], the present water uptake was independent of the two temperatures for the three geometries of samples investigated (cf. Table 3).

Although temperature has little, if any, effect on water uptake in the physiological region, an increase in temperature generally decreases the mechanical properties at a given RH or water uptake (cf. Figs. 5–7). Moduli (E_B and E_T) are known to diminish as the glass transition temperature (T_g) is approached [56]. In the present work, conditioning at 37 versus 22°C represents a change that is 15°C closer to the unhydrated T_g of 105°C [51], which has been depressed somewhat, depending upon exactly how much water has been sorbed. Consequently, E_T and ε_{UTS} decreased marginally as temperature increased; whereas, UTS was not significantly different with temperature. Both HK and HV also decreased as temperature increased, presumably because the compliance was greater as the temperature approached the T_g.

Virtually all of the properties tested, except ε (cf. middle right hand frames, Figs. 5–7), displayed a continuous, negative linear dependence as a function of RH or water uptake, thereby supporting the aforementioned first hypothesis. Shen et al. [18] reported from other works that, between 20 and 40°C, PMMA was a semi-brittle polymer having an UTS = 50 − 80 MPa and an ε_F = 0.04 − 0.20, wherein 0.04–0.08 was the norm. The present UTS values are not as low, and ε_F values can be much higher than 0.20, which suggests that residual stresses associated with non-equilibrium conditions may have been at work. For a commercial grade PMMA (Perspex) and a dental polymer, Smith [22] found that strength decreased by 8.4 and 8.9% after 14 d in water at 37°C. This time frame was not an equilibrium condition, and internal stresses surely were generated. Similarly Shen et al. [18] reported a decrease from 69.4 to 48.8 MPa in their dry and wet states (here their effective %RHs were unknown), which represented a change of 30%. In the present work, UTS decreased from 75.7 to 60.7 MPa or from 76.0 to 58.6 MPa (Table 4) for a change of 20 or 23%, respectively. Also in Shen et al. [18], ε_F reportedly decreased from 0.15 to 0.07 in their dry and wet states, respectively. This anti-plasticization effect was explained by invoking both plasticization and clustering. Below an uptake of ca 1%, the water was sequestered as individual molecules and plasticized the structure; above ca. 1%, the water clustered and acted more as a filler than as a plasticizer. When clustering occurred, haziness appeared,

Table 5
Summary of the mechanical properties of as-received samples

Conditioning temperature (°C)	Actual relative humidity (%)	For the dumbbell specimens			
		Modulus, E_T (GPa)	Ultimate tensile strength, UTS (MPa)	Strain at UTS, ε_{UTS} (mm/mm $\times$100)	Knoop Hardness, HK (kg/mm^2)
22	0	2.90 ± 0.29[a]	77.6 ± 1.2	7.1 ± 0.4	22.0 ± 0.4
	13	2.93 ± 0.12	73.5 ± 1.1	6.8 ± 0.1	21.8 ± 0.5
	33	2.98 ± 0.10	75.5 ± 0.3	6.9 ± 0.1	21.0 ± 0.5
	54	2.95 ± 0.10	72.9 ± 0.8	6.8 ± 0.2	20.3 ± 0.2
	76	2.51 ± 0.08	66.7 ± 1.7	6.8 ± 0.2	19.0 ± 0.5
	86	2.63 ± 0.10	66.6 ± 0.6	7.3 ± 0.3	18.4 ± 0.5
	93	2.43 ± 0.07	61.8 ± 2.0	7.1 ± 0.2	18.9 ± 0.4
	100	2.39 ± 0.11	61.6 ± 0.9	7.1 ± 0.3	17.0 ± 0.4
37	0	2.78 ± 0.10	77.0 ± 1.0	6.7 ± 0.5	21.6 ± 0.3
	12	2.89 ± 0.08	75.6 ± 0.4	6.7 ± 0.1	20.9 ± 0.3
	32	2.84 ± 0.09	72.8 ± 0.6	6.7 ± 0.1	19.6 ± 0.7
	49	2.72 ± 0.09	71.9 ± 0.5	6.7 ± 0.2	19.4 ± 0.8
	75	2.54 ± 0.14	65.8 ± 0.2	6.7 ± 0.4	18.4 ± 0.8
	83	2.49 ± 0.07	66.6 ± 0.3	6.9 ± 0.2	18.1 ± 0.6
	90	2.59 ± 0.10	65.5 ± 1.2	6.5 ± 0.2	18.4 ± 0.4
	100	2.41 ± 0.12	61.4 ± 0.4	6.7 ± 0.2	16.8 ± 0.5

[a] Means ± standard deviation are reported for six data points.

and significant changes in the deformation response resulted.

Under equilibrium conditions, the present effort shows no evidence to sustain the argument that a discontinuity between plasticization and clustering exists, which consequently has different effects on the mechanical properties. All samples appeared transparent, regardless of %RH. All mechanical properties (cf. Figs. 5–7) were continuous functions. Except for the somewhat more scattered modulus data that was obtained using the 50% extensometer at 37°C (cf. ∇ data in the upper right hand frames of Figs. 5 and 6), the moduli (E_B or E_T), strength (UTS), and hardness (HK or HV) data resulted in linear regressions that were highly significant ($p < 0.001$). For the measures of strain (ε_{UTS} and ε_F), the outcomes were quite logical, too. The ε_{UTS} was independent of RH or uptake. When this data and the UTS were combined, the secant modulus (E_{SEC}) plotted as a continuous function (not shown), further disputing the aforementioned second hypothesis. Indeed, the ε_F had a continuous, positive dependence, which suggested that further plasticization was proceeding with each successive increment of water. Judging by the inherent scatter of such data, however, ε_F was quite sensitive to inherent flaws even under equilibrium conditions, as they also had to be under internal stress while equilibrium conditions were being attained. Nonetheless, the values of ε_F increased significantly ($p < 0.02$) with water uptake — in those least ductile specimens the values still nearly doubling from 0.06 to 0.11 as the sorption proceeded from 0 to 2.1% (cf. middle right hand frame, Fig. 6).

These earlier observations may be explained by recalling the conditioning procedures. Previous workers often placed samples at 0 or 100% RH for specified times to attain not only 0 and 100% hydration but also all intermediate values. If the residence time was sufficient, the 0 and 100% RH conditions were representative of the boundary conditions. Otherwise, these would have internal strains present, too. As water sorption begins, the internal stresses build-up as the strain differential across the sample increases. During this build-up, the sample is becoming plasticized, which reduces the nucleation stress for crazing. At some critical compositional gradient, the combination of internal stress and plasticization is such that micro-crazed regions nucleate. These defects cause the hazy appearance, which has been alluded to by some investigators, as water aggregates within some of these regions. But regardless, the defects so generated at ca. 1% sorption result in the apparent discontinuities of the mechanical properties. As even the present equilibrium conditions have shown, these plasticized materials can become sensitized to defects as water uptake progresses and will fail over a broad range of strains, if such defects are nucleated during conditioning. In the final analysis, clustering may occur, but only because the defects that host it were produced as an artifact during conditioning. The practical ramifications of this analysis is that the sorption of water can damage the structure and reduce the mechanical properties mentioned here as well as compromise the wear [11,12,31] and fatigue [29,30] properties that are so important to adequate service.

4.3. Modeling and presentation of interrelationships

In less conventional terms, amorphous PMMA may be modeled as a partially covalently bonded but highly disorganized crystalline material in which only one-third of the primary bonds of a three-dimensional (3D) lattice exist and

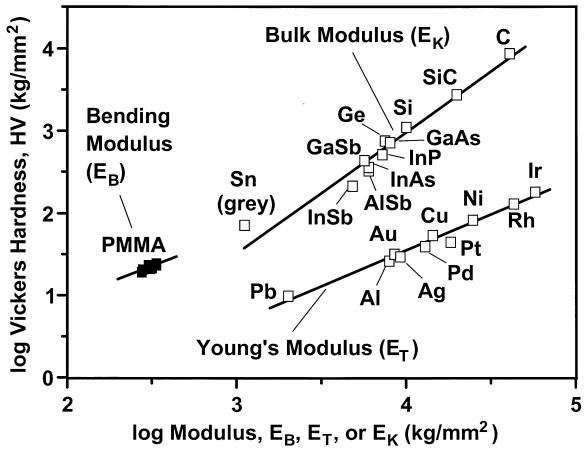

Fig. 9. Relationships of HV to moduli (E_B, E_T, or the bulk modulus [E_K]) for annealed PMMA ($p < 0.02$), face-centered-cubic metals (FCC; $p < 0.001$) [66], and covalent crystals ($p < 0.001$) [66], respectively.

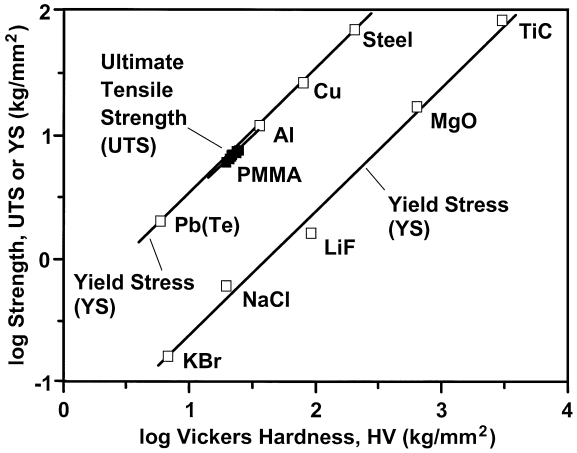

Fig. 10. Relationships of strengths (UTS or YS) to HV for annealed PMMA (using the UTS) and for FCC metals [66,67] and ionic crystals [66,67] (using the yield strength, YS). Each of these regressions were highly statistically significant ($p < 0.001$).

in which only short-range order initially prevails. These last two descriptors preclude the usual barriers that obstruct three-dimensionally bonded covalent solids from deforming. Thus, within this amorphous material, deformation occurs along the remaining two-thirds of the weaker van der Waals bonds without lattice constraints involving specific stereographic positioning. In a classic covalent crystal such lattice constraints would result in the formation of a 3D network, which would limit plastic deformation as it emulates a highly crosslinked polymer [57]. In PMMA, however, deformation is facilitated either by self-diffusion or dislocation motion. In principle, self-diffusion can occur by reptation along the long-axis of each molecule [58]; whereas in the broadest sense, dislocation motion can occur but the slip systems and the Burgers vectors would vary considerably [59]. Ultimately, water should further facilitate the rate at which deformation occurs in PMMA via the depression of the T_g from plasticization [5,16,17,60].

Because the covalent character of the PMMA molecules can be circumvented by these deformation mechanisms, hydrated PMMAs should behave more like materials that have facile deformation mechanisms available — that is, more like the pure, face-centered-cubic (FCC) materials. In materials such as gold, nickel, and irridium, the prerequisite five slip systems are available [61] so that dislocation glide and plastic deformation can readily occur. Flow is only limited by the rate at which dislocations tangle and strain hardening occurs. Rice [62] has shown that, if the primary and secondary slip systems are equally facile, the YS/HV equals 0.33; whereas, as the secondary systems increasingly become more sessile, this fraction progressively decreases to 0.03.

To test this model, correlations of hardness with modulus and strength were sought. The rationale here is that the resistance of a material to plastic deformation (via hardness) [63] is related to the slope of its fundamental binding force-separation distance (modulus) [64] and the demarcation point above which its cohesive failure (strength) ultimately occurs [65]. In other words, the proposition is that hardness measurements can elucidate both the elastic and plastic character of plasticized PMMA.

Figs. 9 and 10 illustrate that water-plasticized PMMA specimens mimic the facile deformation, which is observed in FCC metals [66,67] (cf. also Figs. 13 [66,68], 17 [66,69], and Figs. 1 and 2 of Abson et al. [70]). In the annealed precondition, a linear correlation was found between log HV versus log E_B ($p < 0.02$; Fig. 9). These results paralleled other work noted on plastics [71] and the relationship found for pure FCC metals ($p < 0.001$) in which the slope equaled 0.88 in contrast to the slope of 1.5 for covalent crystals ($p < 0.001$) [66]. The offset of the PMMA data relative to the FCC data is logical on the basis that, in PMMA, plastic deformation occurs only within a localized band [72,73]. For the present 12.7 mm gage length, the bulk of the deformation would occur in a craze some two wavelengths of red light thick (13,000 Å) [72,74], resulting in an apparent strain measurement that would only be but a fraction of expectations. Nonetheless, the current slope of 0.80 for PMMA supports the premise that hydrated PMMA parallels the elastic model of pure FCC metals for long-range elastic interactions, which are facilitated in PMMA by water. Although not shown, highly significant ($p < 0.01$) slopes of 0.85 and 0.90 were also obtained for log HK versus log E_B in the annealed and as-received conditions, respectively.

In a second interrelationship, the log strength strongly correlated with the log HV ($p < 0.001$) and was coincident with the relationship for pure FCC metals (Fig. 10). For hydrated PMMA in the annealed precondition and for FCC metals, the slopes equaled 0.31 and 0.35, respectively [66,67]; for ionic crystals, the slope was 0.03 [66,67]. When the log strength versus log HK were considered in the annealed and as-received precondition (not shown), the

slopes equaled 0.42 and 0.57, respectively ($p < 0.001$). These outcomes illustrate that plastic anisotropy (i.e. the situation that exists when deformation properties differ with orientation [75]) is not prevalent in hydrated PMMA. Indeed, hydrated PMMA follows a model of plastic isotropy that parallels more closely the model for pure FCC metals than one for simple covalent or ionic crystals. Nearly sixty years ago, Souder and Paffenberger first showed that such a relationship exists between hardness and UTS for FCC dental alloys [53]. Now we suggest that the concept may be extended to hydrated PMMA as well.

5. Conclusions

From the foregoing experiments on rectangular parallelepipeds, dumbbells, and disks of PMMA that were equilibrated at eight relative humidities (RH), the following were adduced:

1. Saturation of 1.5 mm thick samples occurs after two months, regardless of RH.
2. Water uptake in PMMA is 2.1% w/w, when specimens are pre-conditioned to the dry state prior to hydration in water.
3. Although temperature changes within the physiologic range of interest have little, if any, effect on water uptake, increased temperature marginally decreases most mechanical properties.
4. Mechanical properties in bending (modulus), tension (modulus and ultimate tensile strength), and hardness (Knoop and Vickers) have a continuous, negative linear dependencies with RH or water uptake; whereas, strain at break has a continuous, positive dependence. Under these equilibrium conditions, there is no evidence to sustain the argument that the division between plasticization and clustering at 1% uptake has different affects on the mechanical properties.
5. Among the mechanical properties tested, only strain at the ultimate tensile strength is independent of RH or uptake. Given the dependence of the UTS (cf. conclusion (4)), the secant modulus will display a negative dependence, too, further substantiating that the properties follow a continuous function.
6. Annealed and as-received specimens give the same outcomes (cf. conclusions (4) and (5)), thereby suggesting that the plasticization afforded by hydration can largely accommodate their differences in internal strains.
7. A positive, linear dependence exists between hardness and modulus for not only covalent crystals and fcc metals but also for hydrated PMMA, which suggests some semblance between the outcomes caused by the deformation kinetics of ductile metals and the plastic zone of this hydrated glassy polymer.
8. A positive, linear dependence exists between strength and hardness for not only ionic crystals but also for fcc metals and PMMA, in which the latter two are collinear.

Acknowledgements

This paper is dedicated to the memory of Dr Derek, T., Turner, who loved this watery science and routinely shared his keen wit. This research was also supported, in part, by PHS NIH NIDR DE06201.

References

[1] Glenn JF. Dental polymers. In: Gebbelein CG, Koblitz FF, editors. Biomedical and dental applications of polymers. New York: Plenum, 1981. p. 317–35.
[2] Stafford GD, Smith DC. Brit Dent J 1968;125:337–42.
[3] Stafford GD, Smith DC. Brit Dent J 1968;125:529–33.
[4] Miettinen VM, Vallittu PK, Docent DT. J Prosthet Dent 1997;77:531–4.
[5] Kalachandra S, Turner DT. Dent Mater 1989;5:161–4.
[6] Kalachandra S, Kusy RP, Wilson TW, Shin ID, Stejskal EO. J Mater Sci: Mater Med 1993;4:509–14.
[7] Nazhat SN, Parker S, Braden M. J Dent Res (Abstr #832) 2000;79:247.
[8] Paffenbarger GC, Rupp NW. Int Dent J 1974;24:1–11.
[9] Asmussen E, Scand J. Dent Res 1984;92:257–61.
[10] Braden M, Clarke RL. Biomaterial 1984;5:369–72.
[11] Solderholm K-J, Zigan M, Ragan M, Fischlschweiger W, Bergman M. J Dent Res 1984;63:1248–54.
[12] McKinney JE, Wu W. J Dent Res 1985;64:1326–31.
[13] Brauer GM, Sweeney WT. Modern Plastics 1955;32:138–43.
[14] Braden M. Brit Dent J 1963;31:83–8.
[15] Gilbert AS, Pethrik RA, Phillips DW. J Appl Polym Sci 1977;21:319–30.
[16] Hargreaves AS. J Dent 1978;6:342–52.
[17] Ristic B, Carr L. J Prosthet Dent 1987;58:689–93.
[18] Shen J, Chen CC, Sauer JA. Polymer 1985;26:511–8.
[19] Smith DC. Brit Dent J. 1958;105:86–91.
[20] Barsby MJ, Braden M. J Dent Res 1979;58:1581–4.
[21] Barsby MJ. J Dent 1992;20:240–4.
[22] Smith DC. Brit Dent J 1961;111:9–17.
[23] Dixon DL, Ekstrand KG, Breeding LC. J Prosthet Dent 1991;66:510–3.
[24] Heath JR, Boru TK, Grant AA. J Oral Rehabil 1993;20:517–24.
[25] Cucci AL, Vergani CE, Giampaolo ET, Afonso MC. J Prosthet Dent 1998;80:434–8.
[26] Vallittu PK. J Dent Res (Abstr #827) 2000;79:247.
[27] Woelfel JB, Paffenbarger GC, Sweeney WT. J Am Dent Assoc 1963;67:489–504.
[28] Tsuruta S, Viohl J. Dent Mater J 1996;15:51–7.
[29] Fujii K. Dent Mater J 1989;8:243–59.
[30] Smith DC. Brit Dent J 1961;110:257–67.
[31] Wu W, Toth EE, Moffa JF, Ellison JA. J Dent Res 1984;65:675–80.
[32] Arima T, Murata H, Hamada T. J Oral Rehabil 1996;23:476–80.
[33] Cornejo-Bravo JM, Siegel RA. Biomaterial 1996;17:1187–93.
[34] Iwami Y, Yamamoto H, Sato W, Kawai K, Torii M, Ebisu S. Operative Dent 1998;23:132–7.
[35] Patel R, Braden M, Patel MP. J Dent Res (Abstr #833) 2000;79:248.
[36] Kalachandra S, Turner DT. Polymer 1987;28:1749–52.
[37] Parker S, Martin D, Braden M. Biomaterial 1999;20:55–60.
[38] Dhuru V, Benhamuerlaine M. J Dent Res (Abstr #1100) 2000;79:281.
[39] Gorthy JM, Oshida Y, Moore BK. J Dent Res (Abstr #1096) 2000;79:280.
[40] Dominguez NE, Thomas CJ, Gerzina TM. Int J Prosthet 1996;9:137–41.
[41] McCabe JF. Anderson's applied dental materials. 6th ed. Oxford: Blackwell Scientific, 1985 (p. 90).
[42] Braden M. J Prosthet Dent 1964;14:307–16.

[43] Braden M, Causton EE, Clarke RL. J Dent Res 1976;55:730–2.
[44] Kusy RP, Lee HB, Turner DT. J Mater Sci: Lett 1977;12:1694–6.
[45] Kusy RP, Turner DT. Polymer 1976;17:161–6.
[46] O'Brien FEM. J Sci Inst 1948;25:73–76.
[47] Dean JA, editor. Lange's handbook of chemistry 15th ed. New York: McGraw-Hill, 1999. p. 116.
[48] Wachtman JB, Capps W, Mandel J. J Mater 1972;7:188–94.
[49] Morena R, Beaudreau GM, Lockwood PE, Evans AL, Fairhurst CW. J Dent Res 1986;65:993–7.
[50] Ban S, Anusavice KJ. J Dent Res 1990;69:1791–9.
[51] Loshaek S. J Polym Sci 1955;15:391–404.
[52] Kusy RP, Turner DT. J Dent Res 1974;53:501.
[53] Souder W, Paffenberger GC. Physical properties of dental materials. Washington, DC: USA Gov't Printing Office, 1942 (p. 64).
[54] Hoff EW. J Appl Chem 1952;2:441–8.
[55] Phillips RW. Skinner's science of dental materials. 7th ed. Philadelphia, PA: WB Saunders, 1973 (p. 202).
[56] Nielsen LE. Mechanical properties of polymers. New York: Reinhold, 1962 (p. 178).
[57] Aklonis JJ, MacKnight WJ, Shen M. Introduction to polymer viscoelasticity. New York: Wiley-Interscience, 1972 (p. 37–43).
[58] DeGennes PG. J Chem Phys 1971;55:572–9.
[59] Li JCM, Gilman JJ. Theories of microstructural defects. In: Baer E, Radcliffe SV, editors. Polymeric materials: relationships between structure and mechanical behavior. Metals Park, OH: American Society for Metals, 1975. p. 239–76.
[60] Patel MP, Braden M. Biomaterial 1991;12:653–7.
[61] Johnston WG. Deformation mechanisms of refractory and other materials: report #ARL 65-135. Aerospace Research Laboratories, OAR, US Air Force, undated literature.
[62] Rice JR. Hardness — a strength microprobe Private communication as reported by Gilman, J.J. In: Westbrook JH, Conrad H, editors. The science of hardness testing and its research applications. Metals Park, OH: American Society for Metals, 1973. (p. 57–8).
[63] Newby JR. Metals handbook, Mechanical testing. 9th ed., vol. 8. Metals Park, OH: American Society for Metals, 1985 (p. 90–113).
[64] Shackelford JF. Introduction to materials science for engineers, 4th ed. Upper Saddle River, NJ: Prentice-Hall, 1996. (p. 274–5).
[65] Jastrzebski ZD. The nature and properties of engineering materials. 2nd ed. New York: Wiley, 1976 (p. 265–70).
[66] Gilman JJ. Hardness — a strength microprobe. In: Westbrook JH, Conrad H, editors. The science of hardness testing and its research applications. Metals Park, OH: American Society for Metals, 1973. p. 51–74; also p. 120–3.
[67] Westbrook JH. Flow in rock-salt structures: report #58-RL-2033. G.E. Research Laboratory, August, 1958.
[68] Clark Jr. SP, editor. Handbook of physical constants: memoir #97. Geological Society of America, 1966.
[69] Cline CF, Kahn JS. J Electrochem Soc 1963;110:773.
[70] Abson DJ, Kosik O, Uvira JL, Jonas JJ. Correlations between room-temperature hardness and flow stress in hot worked metals. In: Westbrook JH, Conrad H, editors. The science of hardness testing and its research applications. Metals Park, OH: American Society for Metals, 1973. (p. 91–8).
[71] Haward RN. The strength of plastics and glass. London: Interscience, 1949 (p. 138).
[72] Berry JP. J Polym Sci 1961;50:107–15.
[73] Kusy RP, Turner DT. Polymer 1977;18:391–402.
[74] Kusy RP, Katz MJ. Polymer 1978;19:1345–57.
[75] Van Vlack LH. Elements of materials science and engineering. 6th ed. Reading, MA: Addison-Wesley, 1989 (p. 254–5).